Vol 16 No 11, November 2007
1009-1963/2007/16(11)/3520-16
Chinese Physics
© 2007 Chin. Phys. Soc.
and IOP Publishing Ltd

Origin of magnetization-induced anisotropy of magnetic films*

Jin Han-Min(金汉民)[a)b)†], Chong-Oh Kim[a)], Taek-Dong Lee[c)], and Hyo-Jin Kim[d)]

[a)] *Research Center for Advanced Magnetic Materials, Chungnam National University, 220, Gung-dong, Youseong-gu, Daejeon 305-764, RO Korea*

[b)] *Department of Physics, Jilin University, Changchun 130023, China*

[c)] *Department of Materials Science and Engineering, Korea Advanced Institute of Science and Technology, 373-1, Kusong-dong, Youseong-gu, Daejeon 305-704, RO Korea*

[d)] *Department of Materials Science and Engineering, Chungnam National University, 220, Gung-dong, Youseong-gu, Daejeon 305-764, RO Korea*

(Received 18 October 2006; revised manuscript received 23 July 2007)

It is proposed that the magnetization-induced anisotropy of magnetic films of cubic crystal structure originates from the anisotropy of atomic pair ordering, shape anisotropy, and strain anisotropy resulting from the constraint of the magnetostriction strain imposed on the film by the substrate. Calculated are the three anisotropy constants and their sum K vs temperature for Ni, Fe, and 55%Ni–Fe films; the room temperature (RT) constants vs the substrate temperature T_t during deposition or annealing after deposition for Ni and 50%Ni–Co films; the RT constants vs composition fraction for Fe–Ni films with T_t = RT, 250 °C and 450 °C, Co–Ni films at T_t = RT, 100 °C and 320 °C, and Fe–Co films with T_t = RT and 300 °C; the spread of RT K vs composition fraction for Fe–Ni films; and RT $\Delta K/K$ vs composition fraction for Fe–Ni and Co–Ni films, where ΔK denotes the variation of K of the film that is detached from its substrate. The calculated curves well accord with the measurements. The irrelevancy of K to the substrate material and the fast kinetics of the annealing in a field applied in the direction of the hard axis are explained reasonably.

The anisotropies of Fe and Ni films originate mainly from the shape anisotropy and the strain anisotropy, respectively. The major anisotropy component in many cases depends not only on composition fraction but also on T_t . For example, the RT anisotropy of 40−70%Ni–Fe films, when T_t is RT, mostly comes from the anisotropy of atomic pair ordering while it stems mostly from the shape anisotropy when T_t is 450 °C. The most important cause of the spread in values of K is the spread of the intrinsic anisotropic stresses superimposed on the intrinsic isotropic planar stress. It is suggested that the field cooling induced magnetic anisotropy originating from the induced crystal texture observed in the bulk alloys is also a major origin for Co and Co-rich alloy films of hexagonal crystal structure.

Keywords: magnetization-induced anisotropy, magnetic film
PACC: 7530G, 7570

1. Introduction

If a magnetic film is deposited at normal incidence in a magnetic field H_t applied in the film plane (by any means such as evaporation, sputtering, electrodeposition, etc.) or annealed in the field after deposition, an in-plane uniaxial anisotropy is induced with an easy direction (ED) in the field direction.[1−5] The anisotropy is magnetization-induced anisotropy, and the function of the field is simply to align the magnetization uniformly.[5−9] The anisotropy is an important fundamental property of the magnetic films and plays an important role in many applications including information storages and sensors.[10,11]

The characteristics of the anisotropy have been studied comprehensively in the 1960s. A number of systematic experimental data have been accumulated. The data include the anisotropy constant K as a function of composition, substrate temperature during deposition or annealing, T_t, and measuring temperature T for Fe–Ni,[8,12−21] Co–Ni[20−22] and Fe–Co[20,22,23] films, K as a function of annealing time during annealing in a field applied in the hard direction (HD) or in a rotating field,[9,15,16,18,20,24−30] and effects of the substrate material on K.[16,20,26,31] K is strongly dependent upon film composition, T_t and T, and it is also affected by other details of experiments, causing in many cases a large spread of experimental data for a given composition, T_t and T.

*Project supported by the Research Center of Advanced Magnetic Materials of Chungnam National University and Korea Research Foundation.
†Corresponding author. E-mail: jinhanmin2000@yahoo.com

The physical essence of the anisotropy has been extensively explored in the same period, and various mechanisms have been suggested accordingly. Many investigators have considered the anisotropy of atomic pair ordering and the strain anisotropy resulting from the constraint of the magnetostriction strain imposed on the film by the substrate to be two major sources of the anisotropy compared with the others.[5,8,9,14,18,20,32–34]

The pair ordering anisotropy constant for binary alloys has been calculated using either the Néel–Taniguchi's expression[35–37]

$$K_{\mathrm{u}}(T) = Gc^2(1-c)^2 J_{\mathrm{s}}^2(T) J_{\mathrm{s}}^2(T_{\mathrm{t}})/T_{\mathrm{t}}, \qquad (1)$$

where G is a constant, J_{s} is the saturation magnetization and T_{t} is in units of K, or Ferguson's empirical expression[38]

$$K_{\mathrm{u}}(\mathrm{RT}) = A(T_{\mathrm{C}} - T_{\mathrm{t}})c^2(1-c)^2, \qquad (2)$$

where $A \approx 55$, c $(0 \le c \le 1)$ is the atomic fraction of one kind of magnetic atoms and T_{C} is the Curie temperature.

The strain anisotropy constant K_λ has been calculated based on either a non-interacting crystallite model or a strongly interacting crystallite model. The former model includes an assumption that there is no interaction between the crystallites and each crystallite is free to deform through magnetostriction to an equilibrium strain during deposition or annealing. If T_{t} is sufficiently high, upon subsequent cooling further deformation occurs and remains so until a certain temperature T_λ below which the mobility of the film atoms on the substrate becomes sufficiently low, causing the film essentially to be constrained to the substrate rigidly. The expression of K_λ has been obtained by averaging the strain energies of the crystallites as

$$K_\lambda(T) = 9[(C_{11} - C_{12})\lambda_{100}(T)\lambda_{100}(T_0) + 3C_{44}\lambda_{111}(T)\lambda_{111}(T_0)]/10, \qquad (3)$$

(in the case of $T < T_\lambda$, $T_0 = T_{\mathrm{t}}$ if $T_{\mathrm{t}} < T_\lambda$, and $T_0 = T_\lambda$ if $T_{\mathrm{t}} > T_\lambda$) where C_{11}, C_{12} and C_{44} are the elastic constants and λ_{100} and λ_{111} the magnetostriction constants.[17] The strongly interacting crystallite model includes an assumption that the adjacent crystallites contact each other and are strongly intercoupled. Different expressions of K_λ have been proposed and/or used. One kind of the expressions is

$$K_\lambda(T) = 3\lambda_{\mathrm{s}}(T)\sigma/2, \qquad (4a)$$

in which $\lambda_{\mathrm{s}} = (2\lambda_{100} + 3\lambda_{111})/5$, σ is the linear stress,[12] or planar stress,[23] or $\lambda_{\mathrm{s}}(T_{\mathrm{t}})E$ (E is the Young's modulus),[14,18,34] or $\lambda_{\mathrm{s}}(T_{\mathrm{t}})E/(1+\nu)$ (ν is the Poisson ratio),[39] or $[\lambda_{\mathrm{s}}(T) - \lambda_{\mathrm{s}}(T_{\mathrm{t}})]E$.[40] Another expression is[32,41,42]

$$K_\lambda(T) = 9\lambda_{\mathrm{s}}(T)\lambda_{\mathrm{s}}(T_0)E(T)/[4(1+\nu)], \qquad (4b)$$

(in the case of $T < T_\lambda$, $T_0 = T_{\mathrm{t}}$ if $T_{\mathrm{t}} < T_\lambda$, and $T_0 = T_\lambda$ if $T_{\mathrm{t}} > T_\lambda$).

As pointed out by West,[17] the values of K_λ calculated by using the two models are quite different from each other for some composition films. For example, for Fe–Ni films with a composition of about 45% Ni the value of room temperature (RT) K_λ with $T_0 = 240\,^{\circ}\mathrm{C}$ calculated from expression (3) is more than twice the value calculated from expression (4b).

With the atomic pair ordering being absent in a pure metal film, the anisotropies of Ni and Fe films have been analysed with a strain anisotropy model. The temperature dependence of K for a Ni film annealed at $400\,^{\circ}\mathrm{C}$[15] was successfully reproduced using expressions (3)[17] and (4b),[42] separately. $K(\mathrm{RT})$ as a function of T_{t} calculated for Ni films, however, is apparently larger than most of experimental data.[32] West has shown that the value of $K(T = T_0 = \mathrm{RT})$ of Fe film calculated from expression (3) coincides with the experimental data but that calculated by expression (4a) with $\sigma = \lambda_{\mathrm{s}}(\mathrm{RT})E$ is about one order in magnitude smaller. He considers the result to be evidence showing that, on the one hand, the anisotropy of Fe films originates dominantly from the strain anisotropy mechanism and, on the other hand, the strongly interacting crystallite model and its K_λ expressions are incorrect.[17]

Several investigators have analysed the experimental data of $K(\mathrm{RT})$ as a function of composition fraction through calculations with the strain model or both of strain and pair ordering combined model (pair–strain model). The films which have been analysed include Fe–Ni,[14,17,18,32] Co–Ni,[34,41] Fe–Co[23,34] and Fe–Co–Ni[22] alloy films. Though many analyses can successfully explain the measurements quasi-quantitatively, a discrepancy between the calculations and the measurements, in general, is apparent, implying that unknown mechanisms remain to be found.

Some insights into the unknown origins come into being after studying the kinetics of annealing process in a HD field (HD annealing) or in a rotating field which eliminates the induced anisotropy.[43]

An apparent change of K was observed for an electrodeposited Ni film after only about 2 min HD annealing at as low as 80 K.[27] Smith *et al*[28] and Kneer and Zinn[44,45] analysed the isotherms of non-magnetostrictive permalloy films ($K_\lambda = 0$) at different temperatures. They have confirmed that a slow process term of activation energy $Q = 1.5$ eV contributes 60% of K value, which is attributed to the pair ordering process. Both research groups have identified several fast process terms of Q between 0.15 eV and 0.5 eV and suggested that an ordering of imperfections may be responsible for the contribution.[45] Iwata and Hagedorn[30] also observed a fast process at the initial stage of HD or rotating field annealing. They considered the fast process as the pair ordering change through diffusion of atoms along the high-diffusivity paths such as grain boundaries and dislocations. An initially very fast change of K during the HD or rotating field annealing is a common phenomenon for the films without being annealed at high temperatures beforehand but the extent of the variation strongly depends on the composition of the film.[16,24–26] If a Fe film deposited at RT is HD annealed at 100 °C, the ED reorientation to the field direction (initial HD) can be completed within a few minutes in contrast to the fact that it takes more than 20 h for 50%Ni–Fe film to achieve its reorientation even at a higher temperature of 200 °C.[16]

Most of the experimental data have not been explained satisfactorily. Many investigators infer that the ordering of impurity atoms and/or imperfections could be responsible for the unknown anisotropies.[5,9,16,20,27,46,47]

A few investigators have analysed the shape anisotropy mechanism.[8,16,42] It is well known that the shape anisotropy is a major origin of the anisotropy of the films deposited at oblique incidence.[7,8] While clear geometrical anisotropy is observed for oblique-incidence films by electron microscopy, no such anisotropy is observed in normal incidence films.[7,48] Crystallites for normal incidence film should also be elongated as shown below, but the shape anisotropy was roughly estimated to be negligibly small by Smith.[8] From the analysis of the temperature dependence of K the shape anisotropy mechanism was also excluded by Takahashi.[16] The same conclusion can be reached through a strict calculation if the widely used traditional approach is taken as explained below. Assume a grain to be of an ellipsoid with a long symmetrical axis in the H_t direction and let V, S and γ denote the grain volume, grain surface area and average grain surface energy, respectively, $d\,(1+\delta)$ and d the dimensions of the major and minor axes, $N_{//}$ and $N_\perp$ the demagnetizing factors of the isolated ellipsoid in the directions of the major and minor axes, respectively, and P the volume fraction of the void, then the relations among V, S, $N_{//}$, $N_\perp$ and δ under the condition of $\delta << 1$ will be expressed as

$$V = \pi d^3(1+\delta)/6, \tag{5}$$

$$S = \pi^{1/3}(6V)^{2/3}(1 + 8\delta^2/45), \tag{6}$$

$$N_{//} \approx 1/3 - 4\delta/15,$$

$$N_\perp = 1/3 + 2\delta/15. \tag{7}$$

As usual, we consider a grain embedded in a film medium with an average magnetization $J_s(1-P)$[49] (Fig.1(a)).

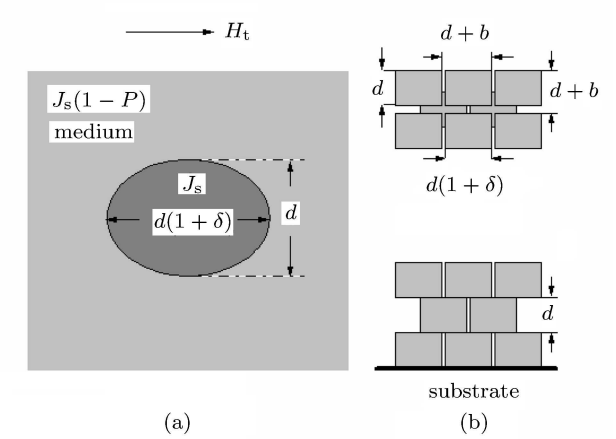


Fig.1. A grain embedded in an average magnetization medium (a) and film model in Ref.[42] (b).

δ at T_t can be obtained by minimizing the sum of the surface energy and demagnetizing energy under the condition of a constant grain volume V, that is,

$$\partial[S\gamma + N_{//}J_s^2(T_t)VP/(2\mu_0)]/\partial\delta = 0, \tag{8}$$

$$\delta(T_t) = J_s^2(T_t)dP/(16\mu_0\gamma). \tag{9}$$

The anisotropy constant at T is

$$K_s(T) = (N_\perp - N_{//})J_s^2(T)P/(2\mu_0)$$
$$= J_s^2(T)J_s^2(T_t)dP^2/(80\gamma\mu_0^2). \tag{10}$$

K_s (RT) = 0.4 J/m^3 for typical parameters of J_s = 1 T, γ = 2 J/m^2, d = 10 nm and P = 0.1, which is about three orders in magnitude smaller than the experimental K value and can be neglected.

Jin[42] has shown that the shape anisotropy is not so small as has been considered. He took a different

approach in the steps after expression (9). By taking into account the fact that the distribution of the grain centres in the film plane is isotropic, he proposed a film model composed of parallelepiped grains with a dimension of $d(1+\delta) \times d \times d$ which are arranged in each grain-layer periodically as shown in Fig.1(b). The centres of the grains constitute a two-dimensional lattice in each grain-layer with the same lattice constants $d+b$ ($b \ll d$) in the directions of major and minor axes. The width of the gap between the neighbouring grains is anisotropic, and is b in the minor axis direction and $b-d\delta$ in the major axis direction. Neglecting the small magnetic field energy stored within the grains, the anisotropy constant is obtained from the difference between the magnetic field energies stored in the gap for the magnetized state along the minor axis direction and major axis direction, that is,

$$\begin{aligned} K_{\rm s}(T) &= [J_{\rm s}^2(T)/(2\mu_0)] \\ &\quad \times [bd^2(1+\delta) - (b-d\delta)d^2]/(b+d)^3 \\ &= J_{\rm s}^2(T)J_{\rm s}^2(T_{\rm t})dP/(32\mu_0^2\gamma), \end{aligned} \tag{11}$$

which is $2.5/P$ times the value obtained from expression (10) and cannot be neglected. He has shown that the experimental curves of K(RT) vs composition fraction and K vs T for Fe–Ni films can be satisfactorily reproduced by using the pair-strain-shape model.[42] The fitted values of $b = 1.6$–2.4 nm, however, seem somewhat too large.

Very limited studies of the induced anisotropy published in recent two decades show that little progress has been made in deepening the insight into the nature of the anisotropy.

The rest of this paper is organized as follows. Section 2 shows that expressions (1) and (2) poorly express $K_{\rm u}$ for deposited films and presents the improved expressions of $K_{\rm u}$, K_λ and $K_{\rm s}$. And Section 3 indicates that the non-interacting crystallite model along with its expression (3) is wrong, and the magnetization-induced anisotropy of the films of cubic crystal structure originates from the pair-strain-shape anisotropy mechanism. Finally some conclusions and discussion are given in Section 4.

2. Model and expressions of anisotropy constants

2.1. Anisotropy constant $K_{\rm u}$ of atomic pair ordering

The theoretical expression (1) is applicable to the alloy in which the atomic pair ordering reaches an equilibrium state at $T_{\rm t}$ and the distribution is maintained at T. The relation is supported by Ferguson's experiments for 50, 60, 70 and 80%Ni–Fe alloys of equilibrium pair ordering at $T_{\rm t}$ in a temperature range between 450 °C and $T_{\rm C}$ (500 °C< $T_{\rm C}$ < 600 °C, $T_{\rm C} - T_{\rm t} \propto J_{\rm s}^2(T_{\rm t})$)[38] as shown in Fig.2(a) (●, ○). Ferguson's empirical expression (2) poorly represents the relation of expression (1) especially for $T_{\rm t}$ lower than 400 °C as shown in Figs.2(a) and 2(b) (▲, ●).

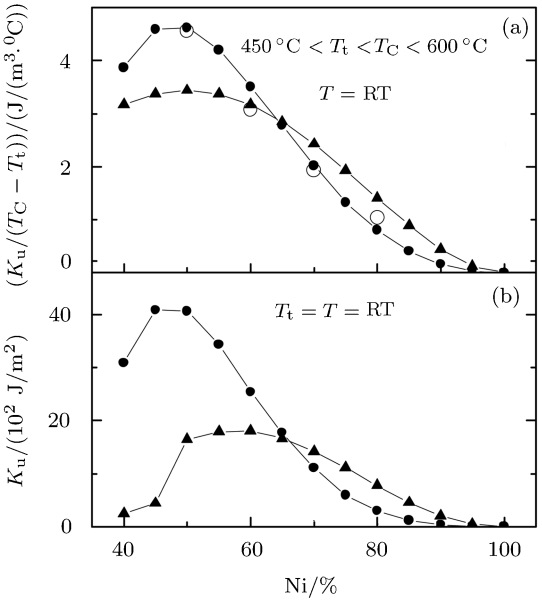


Fig.2. Composition fraction dependences of (a) $K_{\rm u}$(RT)/($T_{\rm C} - T_{\rm t}$) and (b) $K_{\rm u}$(RT) for Fe–Ni alloys. (a) ○: exp.[38], ●: $K_{\rm u}({\rm RT})/(T_{\rm C}-T_{\rm t}) = 29c^2(1-c)^2J_{\rm s}^2({\rm RT})$, ▲: $K_{\rm u}({\rm RT})/(T_{\rm C}-T_{\rm t}) = 55c^2(1-c)^2$. (b) ●: $K_{\rm u}({\rm RT}) = c^2(1-c)^2J_{\rm s}^4({\rm RT})\times 10^4$, ▲: $K_{\rm u}({\rm RT}) = 55c^2(1-c)^2(T_{\rm C}$–RT).

If $K_{\rm Ru} \equiv K_{\rm u}(T = {\rm RT}, T_{\rm t} = T_{\rm u})$ is known, expression (1) can be written as

$$K_{\rm u}(T) = K_{\rm Ru}T_{\rm u}J_{\rm s}^2(T_{\rm t})J_{\rm s}^2(T)/[T_{\rm t}J_{\rm s}^2(T_{\rm u})J_{\rm s}^2({\rm RT})]. \tag{12}$$

Experimental data of $K_{\rm u}$(RT) as a function of composition fraction are available for Fe–Ni and Co–Ni alloy systems. The data for Fe–Ni alloys are the maximum values observed after field cooling from 600 °C at different cooling rates,[50,51] and those for

Co–Ni alloys are obtained after cooling from 1000 °C at a rate of 3.3 °C/min.[52,53] Without the atomic pair ordering reaching an equilibrium state at RT under such treatments, the experimental values do not represent the values for the alloys of equilibrium pair ordering at RT and should be smaller than those with the atomic ordering reaching an equilibrium state at RT. In fact, as shown in Figs.3(a) and 3(b), the experimental composition fraction dependences of the K_u(RT) for Fe–Ni and Co–Ni alloy systems (○) are not proportional to $c^2(1-c)^2J_s^4$(RT) of expression (1) (•), rather, they are approximately proportional to $c^2(1-c)^2$ (▼). For Fe–Co alloys the variation of J_s(RT) with composition fraction is small and $c^2(1-c)^2J_s^4$(RT) ((•) is nearly proportional to $c^2(1-c)^2$ (Fig.3(c)) (▲).

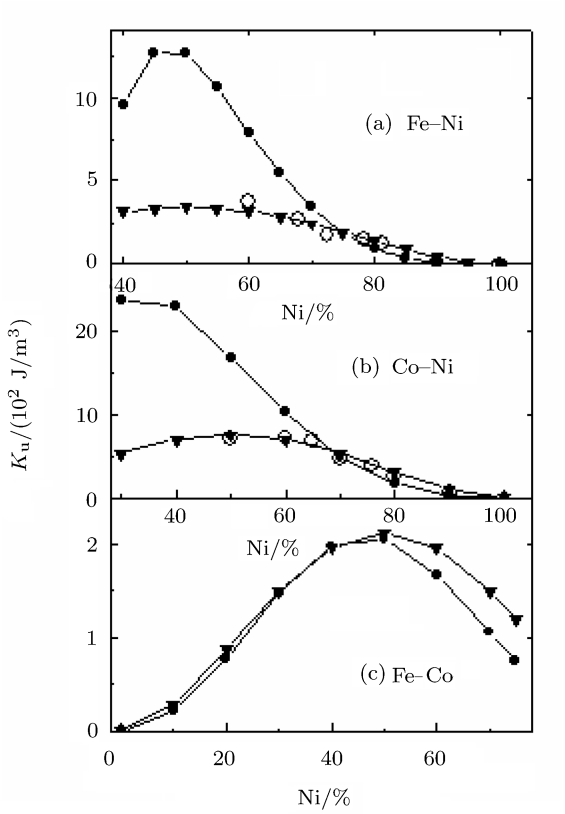


Fig.3. Composition fraction dependences of K_u(RT) for (a) Fe–Ni, (b) Co–Ni and (c) Fe–Co alloys. (a) ○: exp.[50,51], ▼: $K_u = 5.5c^2(1-c)^2 \times 10^3$ J/m^3, •: $K_u = 5c^2(1-c)^2J_s^4$(RT) $\times 10^3$ J/m^3. (b) ○: exp.[52,53], ▼: $K_u = 12c^2(1-c)^2\times 10^3$ J/m^3, •: $K_u = 18c^2(1-c)^2J_s^4$(RT) $\times 10^3$ J/m^3. (c) ▼: $K_u = 3.4c^2(1-c)^2 \times 10^3$ J/m^3, •: $K_u = c^2(1-c)^2J_s^4$(RT) $\times 10^3$ J/m^3.

The duration at T_t for deposited and annealed films is also not long enough to reach an equilibrium pair ordering state and hence the experimental values of K_u of the films are also of non-equilibrium pair ordering state and smaller than those with the pair ordering reaching an equilibrium state. Figure 4 shows K(RT) as a function of composition fraction for Fe–Ni films evaporated at 240–250 °C (□, Δ, ∇). The relation is like $c^2(1-c)^2$ (▼ in Fig.3(a)) with a relatively flat maximum near 50% Ni. After being irradiated by 2 MeV ^{3}He at RT, the around 55% Ni composition film increase the value of K(RT) by several times, transforming the relation into one like $c^2(1-c)^2J_s^2$(RT)$J_s^2(T_t)$ (• in Fig.3(a)) of expression (1) with a sharp maximum (○). The results reveal that the pair ordering which has not reached an equilibrium state in deposited films approaches an equilibrium state through radiation-enhanced diffusion at RT, leading to the dramatic change of the relation between K and composition fraction. The results indicate that expression (1) does not appropriately express K_u, especially K_u vs composition fraction relation, for deposited Fe–Ni and Co–Ni alloy films.

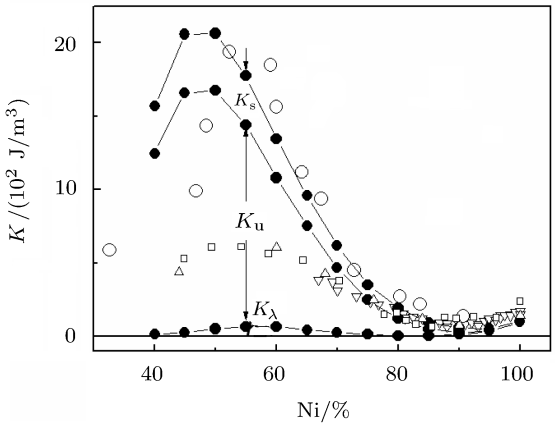


Fig.4. Composition fraction dependences of the calculated RT K_λ, K_u (with respect to K_λ curve, the same meaning hereafter unless otherwise stated), K_s (with respect to $K_\lambda+K_u$ curve, the same meaning hereafter unless otherwise stated) and $K = K_\lambda+K_u+K_s$ (•) and the measured K(RT) for Fe–Ni films evaporated at 240 °C (□[14]) and 250 °C (∇[18], Δ[19]) and irradiated at RT after deposition at 250 °C (○[33]).

Suppose that expression (12) is applicable to the deposited or annealed Fe–Ni and Co–Ni films in which K_{Ru} can be represented by the experimental values of the K_u(RT) of corresponding alloys (▼ in Figs.3(a) and 3(b)), and K_u for the alloy films will be calculated from expression (12). For Fe–Co alloy films and the irradiated Fe–Ni films K_u will be calculated from expression (1). T_u and G are fitting parameters for each alloy film system.

2.2. Shape anisotropy constant K_s

The grains in a film are either granular or columnar as shown in Figs.5(a) and 5(b), respectively.

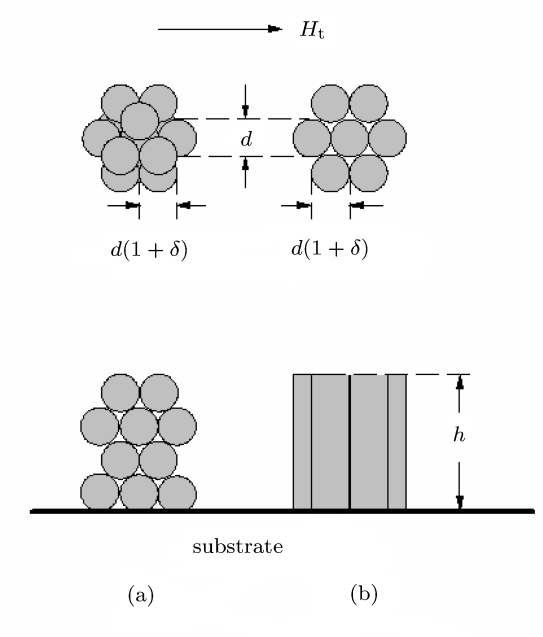


Fig.5. Film composed of (a) granular or (b) columnar grains.

2.2.1. K_s of a film composed of granular grains

Suppose that a grain is of an ellipsoid with a long symmetrical axis in the H_t direction. A grain, on an average, is located in a void of volume $V/(1-P)$ surrounded by a film medium with an average magnetization $J_s(1-P)$. With the distribution of the grain centres in the film plane being isotropic, the section of the void cut by a plane parallel to the film plane is circular as shown in Fig.6 (The grain is in contact with the medium, imitating many adjacent grains partly contacting each other). The magnetic moment interaction between the grain and the surrounding medium is isotropic and affects neither δ nor K_s, and expressions (8), (9) and (10) in which the values of P are all replaced by 1 hold true. K_s, therefore, is simply the shape anisotropy constant of the isolated grains and is

$$K_s(T) = (N_\perp - N_{//})J_s^2(T)/(2\mu_0)$$
$$= J_s^2(T)J_s^2(T_t)d/(80\mu_0^2\gamma), \qquad (13)$$

which is $1/P^2$ times the value obtained from expression (10) and $1/(2.5P)$ times the value calculated from expression (11).

The large differences among K_s values obtained from expressions (10), (11) and (13) appear to be due to the fact that expression (10) is deduced under the implicit assumption of anisotropic distribution of the grain centres in the film plane throughout its derivation, expression (11) is deduced in the same way up to expression (9) and then by assuming isotropic grain centre distribution instead, and expression (13) is derived based on the assumption of isotropic grain centre distribution throughout its derivation.

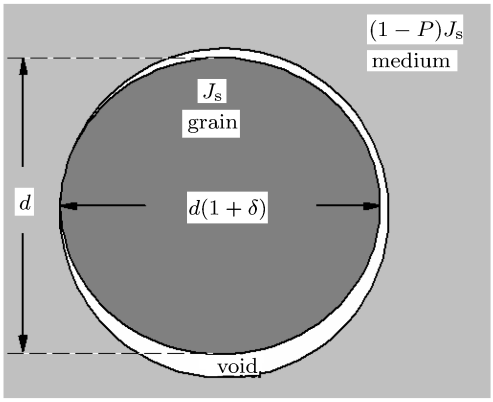


Fig.6. Average circumstance of a grain in a film. For a granular grain film the section is through the centre of the grain.

δ is as small as 2.5×10^{-4} for typical parameters of $J_s = 1$ T, $d = 10$ nm and $\gamma = 2$ J/m^3, justifying the assumption made in expressions (5), (6) and (7). Such a small shape anisotropy cannot be observed by electron microscope. Suppose that a film deposited or annealed at T_t is cooled down to T and kept at the temperature for a long enough time, then some atoms in the side surface of the grain of symmetrical ellipsoid will diffuse toward the two pole side surfaces, resulting in δ changing from $\delta(T_t)$ to $\delta(T)$. The total number of the atoms transferred is

$$n = \pi|J_s^2(T) - J_s^2(T_t)|d^4/(9\sqrt{6}a^3\mu_0\gamma), \qquad (14)$$

where $a \approx 0.356$ nm is the lattice constant of Fe–Ni alloy. The average distance l of the diffusion is roughly one-eighth of the circumference of the ellipsoid. $n \approx 10$ and $l \approx 8$ nm if $d = 10$ nm, and $n \approx 1\times10^5$ and $l \approx 80$ nm if $d = 100$ nm, for typical parameters of $J_s(T_t) = 0.5$ T, $J_s(T) = 1$ T and $\gamma = 2$ J/m^2. The results indicate that K_s of small d film changes very fast through surface diffusion even when the temperature has decreased to a low temperature, and the rate of diffusion decreases dramatically with the increase of d. The same conclusion should be drawn when the film is annealed in a HD or rotating field.

2.2.2. K_s of a film composed of columnar grains

Consider a film composed of columnar grains with elliptical cross section. The dimensions of the long and short axes of the elliptical cross section are $d(1+\delta)$ and d respectively as shown in Fig.5(b). The cross sectional area S and the circumference L respectively are ($\delta \ll 1$)

$$S = \pi d^2(1+\delta)/4, \tag{15}$$

$$L \approx \pi d(1+\delta/2+7\delta^2/16) = 2\sqrt{\pi S}(1+19\delta^2/16). \tag{16}$$

The demagnetizing factors of the isolated columnar grain along the long and short axes in a cross section (the factor is defined by the ratio of the demagnetization field at the centre of the column and the magnetization along the axis direction) respectively are

$$N_{//} \approx \frac{2-[1+2S/(\pi h^2+4S)]\delta}{4\sqrt{1+4S/(\pi h^2)}},$$

$$N_{\perp} \approx \frac{2+[1+(1/2)d^2(1+\delta)/(h^2+d^2(1+\delta)]\delta}{4\sqrt{1+d^2(1+\delta)/h^2}}, \tag{17}$$

where h is the film thickness. The grain, on an average, is situated in a cylindrical void of section $S/(1-P)$ surrounded by the medium with an average magnetization $J_s(1-P)$ (Fig.6). δ is obtained by minimizing the sum of the surface energy and demagnetizing energy under the condition of a constant S as

$$\delta(T_t) = \eta J^2(T_t)d/(76\mu_0\gamma), \tag{18}$$

where

$$\eta = [1+(1/2)d^2/(h^2+d^2)]/\sqrt{1+(d/h)^2}. \tag{19}$$

η increases to 1 monotonically as h/d increases, and exceeds 0.9 at around $h/d=2$ (Fig.7). By taking an approximation of η=1, K_s is given by

$$\begin{aligned} K_s(T) &= (N_{\perp}-N_{//})J_s^2(T)/(2\mu_0) \\ &= J_s^2(T)J_s^2(T_t)d/(152\gamma\mu_0^2), \end{aligned} \tag{20}$$

which is 80/152 times the value obtained from expression (13) of the granular grain film.

The surface energy density of Ni, estimated from the heat of forming gaseous atoms,[54] is 2.6 J/m^2 which is essentially independent of temperature in a temperature range concerned in this work. With the grain boundary energy density being much smaller than this value, a roughly assumed average surface energy γ=2 J/m^2 will be used in the calculations for all films. K_s will be calculated from expression (20) for all films in which d is a fitting parameter.

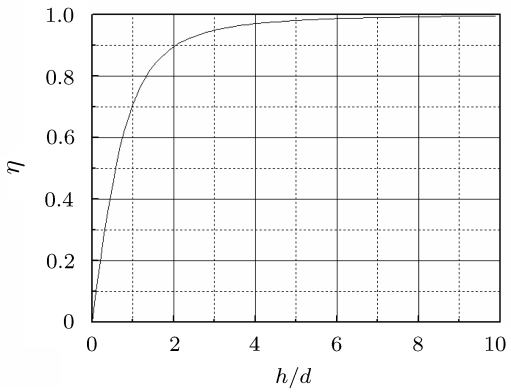


Fig.7. η versus h/d.

2.3. Strain anisotropy constant K_λ

This paper adopts the strongly coupled crystallite model for polycrystalline films. It has been known that there exists an isotropic intrinsic planar stress in a film.[9,23,55–58] It is reasonable to consider the stress to be an ideal isotropic planar stress superimposed by a small anisotropic one. There are also other kinds of stresses. One is the isotropic planar stress arising from different coefficients of thermal expansion of the rigidly coupled film and substrate. Another is the anisotropic stress resulting from the constraint of magnetostriction strain imposed on the film by the substrate. Let $\sigma_{//}$ and $\sigma_{\perp}$ denote the total stress components in the ED and HD directions respectively, then corresponding strain components $a_{//}$ and $a_{\perp}$ will be

$$\begin{pmatrix} a_{//} \\ a_{\perp} \end{pmatrix} = \frac{1}{E}\begin{pmatrix} 1 & -\nu \\ -\nu & 1 \end{pmatrix}\begin{pmatrix} \sigma_{//} \\ \sigma_{\perp} \end{pmatrix}, \tag{21}$$

and the elastic energy will be

$$\begin{aligned} F_\lambda &= \int_0^{a_{script//}} \sigma_{//}\mathrm{d}a_{//} + \int_0^{a_{\perp}} \sigma_{\perp}\mathrm{d}a_{\perp} \\ &= (a_{//}^2 + 2\nu a_{//}a_{\perp} + a_{\perp}^2)E/[2(1-\nu^2)]. \end{aligned} \tag{22}$$

Suppose that the anisotropic intrinsic stress is linear in a direction making an angle ϕ with the ED, and let σ_l denote the stress, $a_{l//}$ and $a_{l\perp}$ the strain components induced by σ_l, a_p total isotropic planar strain, and θ the angle between $\boldsymbol{J}_s$ and the ED, then we will have

$$a_{//} = a_p + a_{l//} + \lambda_s(T_0) - (3/2)\lambda_s(T)(\cos^2\theta - 1/3)$$

and

$$a_\perp = a_p + a_{l\perp} - (1/2)\lambda_s(T_0) - (3/2)\lambda_s(T)(\sin^2\theta - 1/3),$$

and the anisotropy constant is

$$\begin{aligned} K_\lambda &= F_\lambda(\theta = \pi/2) - F_\lambda(0) \\ &= 9\lambda_s(T)\lambda_s(T_0)E(T)/[4(1+\nu)] \\ &+ 3\lambda_s(T)\sigma_l(|\cos\phi| - |\sin\phi|)/2. \end{aligned} \tag{23}$$

(in the case of $T < T_\lambda$, $T_0 = T_t$ for an electrodeposited film and $T_0 = T_\lambda$ for evaporated and sputtered films regardless of T_t)

The first term in the last expression is the same as that in expression (4b) but with a difference in the value of T_0 as given in the parentheses behind the expression. It has been known that the temperature of top surface of a film increases during evaporation.[19] It is conceivable that the temperature of a newly formed cluster (or part of layer) on the film surface decreases from a high temperature due to impinging atoms to T_t during evaporation and sputtering. So in the case of $T < T_\lambda$, it is considered that the relation of $T_0 = T_t$ holds only for electrodeposited films. For the evaporated and sputtered films we assume that $T_0 = T_\lambda$ for all values of T_t. The second term in the last expression (23) is the same as that in expression (4a) in which σ is the difference in σ_l component between the ED and HD.

The temperature dependence of λ_s is not known for most of alloys. λ_s of 78%Ni–Fe varies with temperature nearly linearly,[59] and the rough linear approximation of

$$\lambda_s(T) = \lambda_s(\mathrm{RT})(T_C - T)/(T_C - \mathrm{RT}) \tag{24}$$

will be used for all composition films except pure Fe and Ni films for which the experimental data are available.[60–62] The values of $E(\mathrm{RT}) = 2\times10^{11}$ N/m^2 and $\nu = 0.3$ are both close to those of Fe, Co and Ni,[63] and they will be used for all composition films. The temperature dependence of E is assumed to follow that of Fe[64] (inset in Fig.11) and ν to be approximately independent of temperature for all composition films.

3. Comparison between the theory and experiment

3.1. Normalized remanence as a function of angle between the applied field and ED

Figure 8 shows normalized remanence J_r/J_s as a function of angle θ_H between the ED and an applied field direction in the film plane for a [Fe/Al] multilayer. Let θ denote the angle between $\boldsymbol{J}_s$ and ED. The anisotropy energy of a film composed of strongly exchange coupled nano-crystallites is simply the induced anisotropy energy $K\sin^2\theta$, and the remanence is $\cos\theta_H$ (bold solid curve) in excellent agreement with the measurements (○). The remanence of a non-interacting crystallite is calculated by minimizing the sum of $K\sin^2\theta$ and the crystalline anisotropy energy (two terms of magneto-crystalline anisotropy constants K_1 and K_2). Their average as a function of θ_H (thin solid curve) is not in agreement with the measurements. The results support the strongly interacting crystallite model but not the non-interacting model.

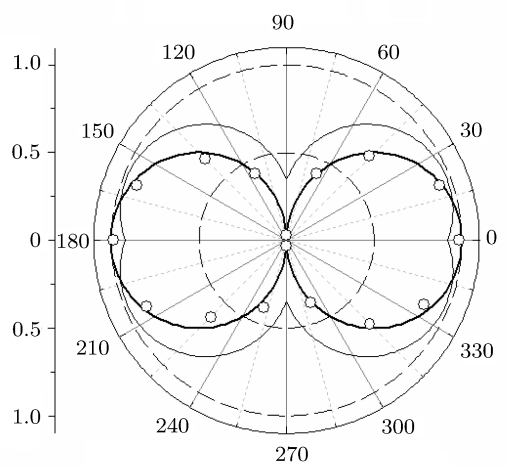


Fig.8. J_r/J_s as a function of θ_H. ○: measured in Ref.[31]. Bold solid curve: calculated from a strongly coupled crystallite model. Thin solid curve: calculated from a non-interacting crystallite model.

3.2. Spread of K as a function of composition fraction for Fe–Ni films

The values of K of the films with the same composition fraction, prepared under the same experimental conditions, are usually very spread.[8,14,18,20,65] Figure 9(a) demonstrates an original experimental data

of K(RT) vs composition fraction for the Fe–Ni films evaporated at 240 °C. The different values of K for a given composition fraction are of three films prepared simultaneously at each evaporation. Figure 9(b) shows the average spread of K,

$$\Delta K = (1/3)\sum_{i}^{1,2,3} |K(i) - \bar{K}|$$

($\bar{K} \equiv (1/3)\sum_i^{1,2,3} K(i)$) (□) and $4.7|\lambda_s(\mathrm{RT})| \times 10^6$ (•) as a function of Ni concentration fraction. The coincidence between the two relations reveals that the spread arises mainly from the spread of K_λ which is proportional to λ_s. As $9\lambda_s(T)\lambda_s(T_0)E(T)/[4(1+\nu)]$ in expression (23) is insensitive to the processing conditions, it is concluded that $\sigma_l(|\cos\phi| - |\sin\phi|)$ should be very sensitive to the growing process of the film and fluctuates in a large range around the average of zero. Since the statistic average of $||\cos\phi| - |\sin\phi||$ is $||\cos\phi| - |\sin\phi||_{\mathrm{av}} = 0.53$, the average value of σ_l, $\bar{\sigma}_l$, is roughly estimated at 6×10^6 N/m^2 from the relation of $\Delta K_\lambda = (3/2)|\lambda_s|\bar{\sigma}_l||\cos\phi| - |\sin\phi||_{\mathrm{av}} = 4.7|\lambda_s| \times 10^6$ J/m^3, which is one to two orders in magnitude smaller than $10^8 - 10^9$ N/m^2 of intrinsic planar stress.[9,23,55]

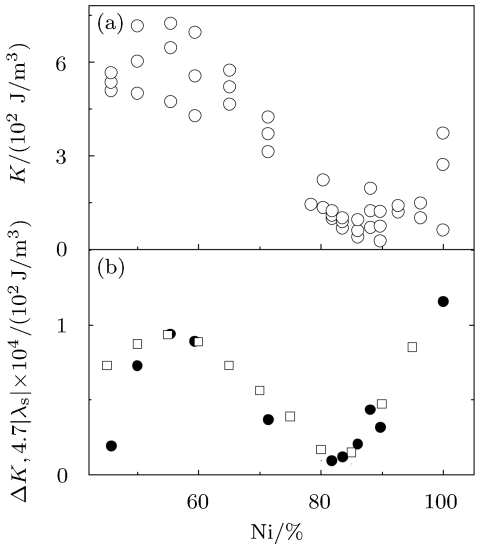


Fig.9. Composition fraction dependences of (a) K (RT),[14] (b) ΔK (□) and $4.7|\lambda_s(\mathrm{RT})| \times 10^6$ (•).

3.3. K(RT) as a function of T_t for Ni films

Figure 10 shows T_t-dependent K(RT) obtained experimentally (separate symbols) and T_t-dependent RT K_s, K_λ and $K = K_\lambda + K_s$ calculated at d = 50 nm (solid symbols + line) for evaporated Ni films. It can be seen that the experimental data are very spread around the average values of $K_s(\mathrm{RT}) + 9\lambda_s(\mathrm{RT})\lambda_s(T_0)E(\mathrm{RT})/[4(1+\nu)]$ with $T_0 = 290$ °C (•). $K_\lambda \gg K_s$ (▼). Apparently the large spread stems from the large spread of $3\lambda_s(\mathrm{RT})\sigma_l(|\cos\phi| - |\sin\phi|)/2$. The average spread is nearly independent of T_t, and the value of $\bar{\sigma}_l$ is estimated at 3×10^6 N/m^2. $K = K_\lambda + K_s$ in which K_λ is calculated from expression (4b) with $T_0 = T_t$ (▲) is larger than the experimental data, and the deviation increases with the decrease of T_t below 290 °C. The results show that the commonly accepted assumption that the magnetostriction is freely strained at T_t when T_t is lower than T_λ (parentheses after expression 4(b))[9,14,17,18,32,33,41] is wrong for evaporated and sputtered films.

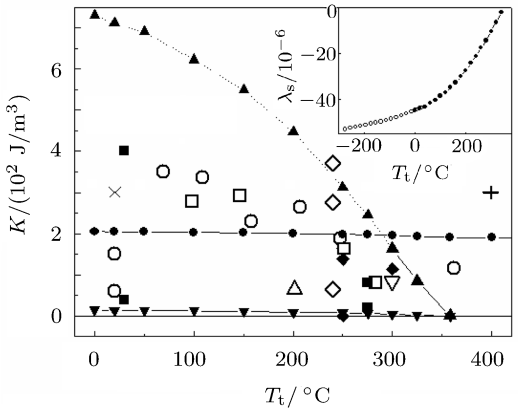


Fig.10. K(RT) vs T_t for Ni films. Exp. :∇[13], ◇[14], +[15], ♦[18], □[19], ×[25], Δ[45], ■[66,17], ○[67]. Calc.: ▼: K_s, • : $K_s + K_\lambda(T_0 = 290\,°\mathrm{C})$, ▲: $K_s + K_\lambda(T_0 = T_t,)$. Inset: λ_s vs T. ○[60,61]. •: renormalized data of Ref.[62] to make the data coincide with the curve of ○ near RT.

In the following the spread is beyond our consideration and the value of $3\lambda_s(T)\sigma_l(|\cos\phi| - |\sin\phi|)/2$ will be taken as the average with zero valued.

3.4. K as a function of T for Ni film

Figure 11 shows the measured (○) and calculated (•) K vs T curves for the Ni film annealed at 400 °C after evaporation. Since $T_t > T_C \approx 360$ °C, we have $K_u = K_s = 0$ and $K = K_\lambda$. The value $T_\lambda = 250$ °C is obtained from the best fit. T_0 is taken as T when T is higher than T_λ on the assumption that the magnetostriction is freely strained when the film is magnetized along the ED at each T before measurement.

The above analyses of the experimental data in Figs.11 and 10 show that T_λ for the Ni film is around

250−300 °C. In the following, the value of $T_\lambda = 300$ °C is used in the calculations for all composition films except that $T_\lambda = 250$ °C, which is also used for better fit in Section 3.12.

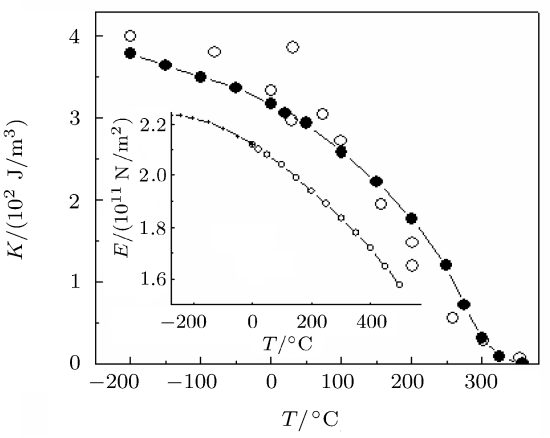


Fig.11. K vs T for Ni film. •: calc., ○: exp.[15]. Inset: E vs T. ○,[64] •: extrapolation of ○.

3.5. K(RT) as a function of composition fraction for Fe–Ni films

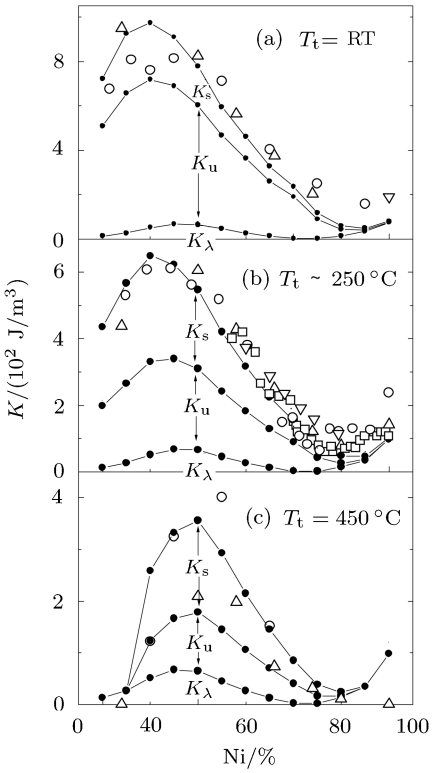


Fig.12. Composition fraction dependences of the calculated RT K_λ, K_u, K_s and K (•) and measured K(RT) (open symbols) for Fe –Ni films (a) evaporated at RT (○[13], Δ[19], ∇: average of the data of Fig.10), (b) 240 °C (○[14]), 250 °C (□[18], Δ[19]), 270 °C (∇[68]), and (c) 450 °C (Δ[19]), and annealed at 450 °C after evaporation at 300 °C (○.[13])

Figures 12(a)–(c) show the composition fraction dependences of the calculated RT K_λ, K_u, K_s and $K = K_\lambda + K_u + K_s$ (•) and the measured K (open symbols) for Fe–Ni films evaporated at RT (a), around 250 °C (b), and 450 °C and annealed at 450 °C after evaporation at 300 °C (c). The calculations are performed with the fitted value of $T_u = 150$ °C for Fe–Ni film system and (a) $d = 20$ nm, (b) $T_t = 250$ °C and $d = 30$ nm, and (c) $d = 40$ nm, respectively.

3.6. K(RT) as a function of composition fraction for irradiated Fe–Ni films

Figure 4 shows the composition fraction dependences of the measured K for the Fe–Ni films irradiated by 2.20 MeV ^{3}He at RT after evaporation at 250 °C (○) and the calculated RT K_λ, K_u, K_s and K with $G = 12 \times 10^5$ J/(m^3·K) and $d = 30$ nm on the assumption that the pair ordering has reached an equilibrium state at RT (•). The calculations coincide with the measurements in a Ni concentration fraction range above 50%, but are apparently larger than the measurements below 50 %. A plausible cause of the disagreement is that the irradiation is not enough for the films of Ni concentration fraction below 50 % to reach an equilibrium state of the pair ordering.

3.7. K as a function of T for Fe film

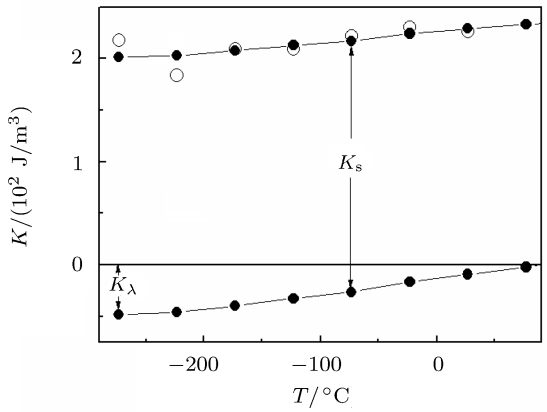


Fig.13. Temperature dependences of the measured K (○[16]) and calculated K_λ, K_s and $K = K_\lambda + K_s$ (•) for the Fe film.

Figure 13 shows the temperature dependences of the measured K of Fe film evaporated at RT (○) and the calculated K_λ, K_s and K with $d = 5.4$ nm (•). K_λ is much smaller than K_s for the film. In striking contrast to the satisfactory reproduction of the measurements by the calculations from expression (23) for

K_λ, the calculations from expression (3) of the non-interacting crystallite model are in complete disagreement with the measurements.[17]

3.8. K as a function of T for 55%Ni–Fe films

Figures 14(a)–(c) show the temperature dependences of the measured K (○) and the calculated K_λ, K_u, K_s and K (•) for 55%Ni–Fe films evaporated at RT (a), annealed at 350 °C (b) and 450 °C (c) after evaporation. The calculations are made with $d = 5.5$ (a), 22.5 (b) and 24 nm (c), separately.

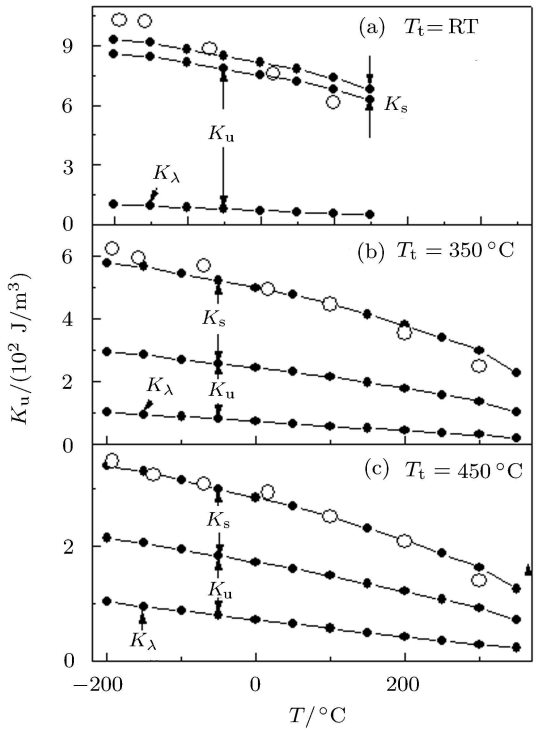


Fig.14. Temperature dependences of the calculated K_λ, K_u, K_s and K (•) and the measured K (○[16]) for the 55%Ni–Fe films evaporated at RT (a), annealed at 350 °C (b) and 450 °C (c) after evaporation at 300 °C.

3.9. K(RT) as a function of composition fraction for Co–Ni films

Figures 15(a)–(c) show the composition fraction dependences of the calculated RT K_λ, K_u, K_s and K (•) and the measured K (RT) for Co–Ni alloy films evaporated at (a) RT (bold curve,[20]) (b) 100 °C (bold curve[21]) and (c) 320 °C (○[22]). The values of λ_s(RT) are cited from Refs.[69,70] and the calculations are performed with the fitted value of $T_u = 400$ °C for the Co–Ni film system and $d = 10$ (a), 11 (b), and 15 nm (c), separately. The inset in subfigure (c) demonstrates that the simulation fails if K_λ is calculated from expression (3) of the non-interacting crystallite model.

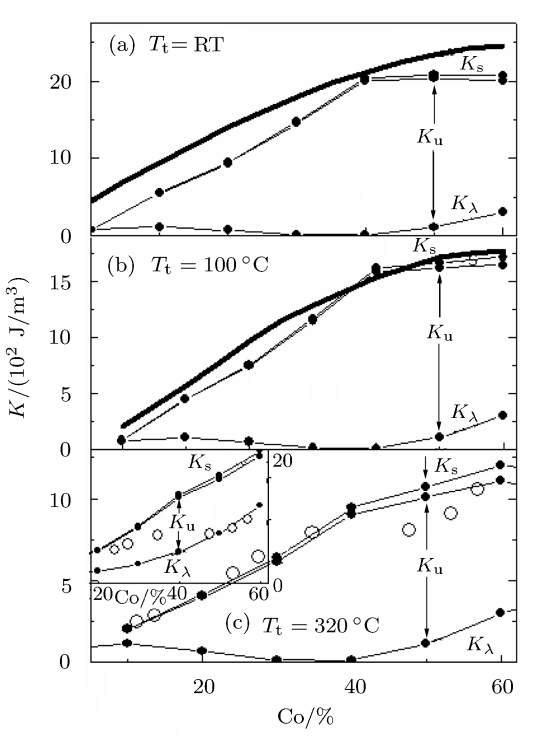


Fig.15. Composition fraction dependences of the calculated RT K_λ, K_u, K_s and K and the measured K(RT) for Co–Ni films. The inset in (c) shows composition fraction dependences of the calculated RT K_λ, K_u, K_s and K (•) in which K_λ is calculated from expression (3). The calculated K_u, K_s and the measured K(RT) (○) are the same as those in (c).

3.10. K(RT) as a function of T_t for 50%Co–Ni films

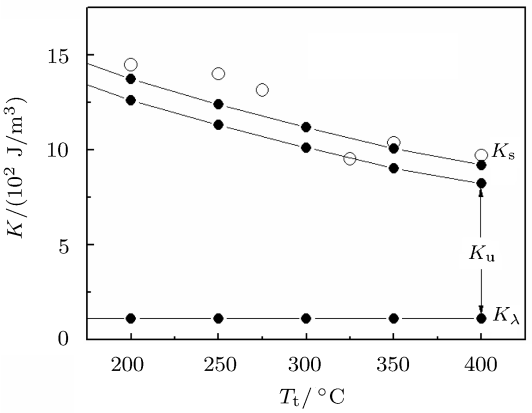


Fig.16. T_t dependences of the measured K(RT) (○[71]) and the calculated RT K_λ, K_u, K_s and K (•) for 50%Co–Ni films.

Figure 16 shows the calculated RT K_λ, K_u, K_s and K (•) and the measured K(RT) (○) for evaporated 50%Co–Ni films. The calculations are made with $d = 25$ nm.

3.11. K(RT) as a function of composition fraction for Fe–Co alloy films

Figures 17(a) and 17(b) show the composition fraction dependences of the calculated RT K_λ, K_u, K_s and K (• + line) and the measured K(RT) for the Fe–Co alloy films electrodeposited (○)(a) and evaporated at around 300 °C (separate symbols) (b). The calculations are made with $G = 3 \times 10^5$ J/(m^3·K) and $d = 40$ nm (a) and $T_t = 300$ °C and $d = 13$ nm (b), separately. The large spread of the measurements of near 52% Co films in subfigure (a) is assumed to be due to the formation of superlattice FeCo.[23] The inset in subfigure (b) shows the measured λ_s(RT) vs Co % and their average (bold solid curve) used in the calculations.

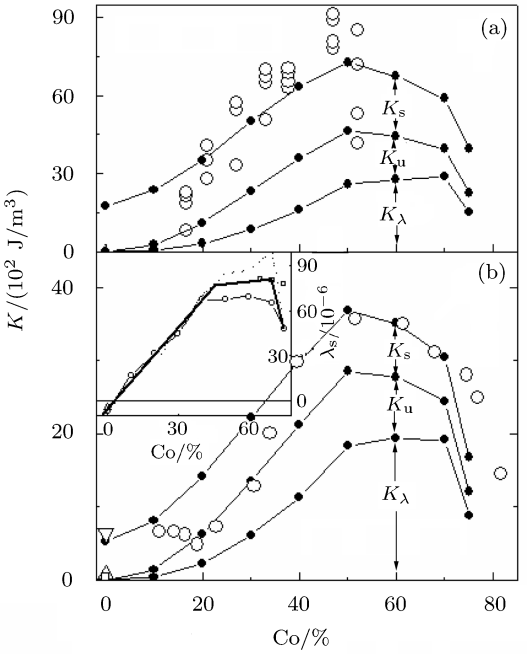


Fig.17. Composition fraction dependences of the calculated RT K_λ, K_u, K_s and K (•) and the measured K(RT) for Fe–Co films electrodeposited at RT (○[23]) (a), and evaporated at 320 (○[22]), 300 (×[72], Δ[73], +[74]), 250–300 (▼[66,17]) and 250 °C (□[20]) (b). The inset in subfigure (b) shows the measured $\lambda_s(RT)$ vs Co% represented by dotted line[75], dashed line[76,77], Δ[78,79], □[80,81] and ○[82].

All the alloy films analysed above are of cubic crystal structure. It has been known that a magnetic anisotropy is induced when a bulk Co metal or a Co-rich Co–Ni alloy is cooled down to RT in an applied magnetic field,[83] which originates from the crystal texture induced by the field cooing through the cubic-hexagonal phase transition temperatures.[84] It is reasonable to consider that the anisotropy is also induced in the films, which is also an important origin of the magnetization-induced anisotropy for the hexagonal-crystal structure Co and Co-rich Co–Ni and Co–Fe films.

3.12. Effects of substrate

Theoretically, K is independent of the thermal expansion coefficient of substrate, which is confirmed by the experimental observations that K is independent of substrate materials with quite different thermal coefficients of expansion (quartz, glass, Mo, etc).[16,20,31] The theoretical prediction that K decreases by $\Delta K = K_\lambda$ if a film is detached from its substrate is confirmed as follows.

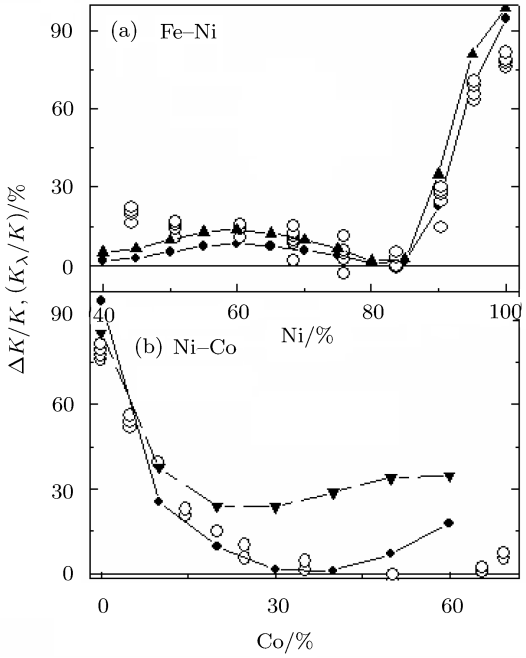


Fig.18. Composition dependences of the measured RT $\Delta K/K$ (○[21]) and the calculated RT K_λ/K (solid symbol+solid line). (a) Fe–Ni films. The calculations are made with $T_\lambda = 300$ °C (•) or $T_\lambda = 250$ °C (▲). (b) Co–Ni films. •: K_λ and K are cited from Fig.15(b); ▼: K_λ are calculated from expression (3) and the K values are the measurements given in Fig.15(b).

Figures 18(a) and 18(b) show the composition fraction dependences of RT $\Delta K/K$ measured for (a) Fe–Ni and (b) Co–Ni films detached from the sub-

strates after evaporation at 100 °C (○) and the calculated RT K_λ/K (solid symbol+solid line). The relations between K_λ/K and composition fraction, calculated with $d = 20$ (•, ▲) in (a) and 11 nm (•) in (b) coincide with the relations between the measured $\Delta K/K$ and composition fraction for the Fe–Ni films and Co–Ni films, respectively.

The relation between $\Delta K/K$ and composition fraction for Co–Ni alloy films has a zero valued minimum near 35 %Co, which is in accord with the case of $K_\lambda = \lambda_s = 0$ for the alloy (Fig.15). If K_λ is calculated from expression (3) of non-interacting crystallites model, K_λ/K never becomes zero and the relation between the calculated K_λ/K and Co concentration fraction (▼) in (b) does not coincide with the measurements (○).

3.13. Kinetics of HD annealing process

Suppose that a film composed of columnar grains is HD annealed at T_t. After annealing for a long enough time the ED rotates to the original HD. The number of the transferred atoms in each atomic layer in the section of the column n and the average distance of the transfer l are

$$n = \pi J_s^2(T_t)d^3/(152a^2\mu_0\gamma) \qquad (25)$$

and roughly $d/8$, respectively. n is as small as 0.065 and $l \approx 4$ nm if $d = 10$ nm, and $n \approx 65$ and $l \approx 40$ nm if $d = 100$ nm for a typical parameter of $J_s(T) = 1$ T. The results indicate that K_s varies very fast through the surface diffusion even at low temperatures for a small d film and the change rate decreases sharply with the increase of d as was also argued about the granular grain film in Section 2.2.1. Such kinetic characteristics of K_s can explain the annealing effects at low temperatures and the fast change of K observed in many films at the beginning of the HD annealing as demonstrated below.

3.13.1. Fe film

Figure 19 shows K(RT) of Fe film evaporated at RT as a function of HD annealing time t at 100 °C. K sharply decreases to negative values, i.e. the ED changes to the original HD within a few minutes. The fast change is expected because K mainly comes from K_s and d is small for the Fe film and K_s varies fast through surface diffusion.

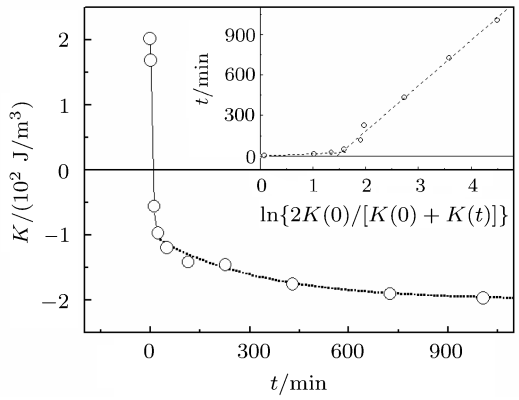


Fig.19. K(RT) vs t for Fe film. ○: measured;[16] line: $K(t) = 1.5[2\exp(-t/\tau_1) - 1] + 0.5[2\exp(-t/\tau_2) - 1]$ in which $\tau_1 = 5$ min and $\tau_2 = 320$ min. Inset: t vs $\ln\{2K(0)/[K(0) + K(t)]\}$.

3.13.2. Ni film

The electrodeposited Ni film after HD annealed for only 2.5 min at as low as 80 K decreases the value of K(80 K) by 14 J/m^3. Apparently the reduction is due to the change of K_s through surface diffusion. If the film is annealed at 400 °C in a field parallel to the ED beforehand, the change decreases to 3.6 J/m^3.[27] The slower decrease is due to the increase of d. The kinetics of HD annealing process at 205 °C for a Ni film evaporated at 205 °C is described by processes featured with three relaxation times of $\tau_1 = 9$ s, $\tau_2 = 440$ s and

$$\tau_3 = 4 \times 10^4 \text{ s}\Big(H_K(t) = \sum_j^n H_j[2\exp(-t/\tau_j) - 1]\Big).$$

The fastest process of $\tau_1 = 9$ s contributes 12 % of $K = 64$ J/m^3.[45] The percentage is in coincidence with the ratio of K_s(200 °C)/(K=64 J/m^3)=0.1 calculated with $d = 50$ nm. K of the Ni film evaporated at RT decreases to zero after a 100 h HD annealing at RT.[15] The long time required to change the ED is expected because it occurs only when the dominant component K_λ of slow process decreases to a value smaller than $2K_s$.

3.13.3. Fe–Ni film

The value of K of 80%Ni–Fe films evaporated at 300 °C is reduced by about 20% within a few seconds during HD annealing at about 220 °C. The fast change is due to the variation of K_s. For 81%Ni–Fe films evaporated at 180 − 200°C the fast process during HD annealing at the same temperature contributes about 40% of K.[28,45] The ratio of K_s/K calculated with

$d = 30$ nm for the same film is also 40%, which shows that the K_s of a film evaporated at about 200 °C still varies very fast. After a 50%Ni–Fe film evaporated at RT has been HD annealed for 70 h at 200 °C, K is reduced by about 90 %, keeping the ED unchanged.[16] The time required to change the ED is comparable with the time taken by the Ni film with T_t being RT to change the ED at RT, that is, K_u changes much slower than K_λ at the same temperature. The ability of 80%Ni–Fe films to be annealed at low temperatures disappears if the film is annealed above 400 °C.[26] These phenomena can be explained by d increasing with the increase of T_t.[9,49,71]

4. Discussion and conclusion

The pair-strain-shape anisotropy model presented in this paper can explain major characteristics of experiments in a broad range reasonably. The simulations of a series of experimental curves are satisfactory though rough approximations are adopted in the calculations and the error of T_t larger than 50 °C is expected in experiments.[19] In Table 1 listed are the values of the fitting parameters T_u and G, T_λ and T_0, and d. Some experimental values of d for evaporated films are also listed in the table for reference. The value of $G = 3 \times 10^5$ J/(m^3·K) for Fe–Co films is expected to be smaller than 13×10^5 J/(m^3·K) for the irradiated Fe–Ni films because of pair ordering in the deposited films poorer than in the irradiated film. The values of T_u and T_λ are larger than RT and in a temperature range of slow diffusion, which seems reasonable. The value of d, in general, increases with the increase of T_t, which is in coincidence with measured one, and the value of d is also in coincidence with the measured value of d in the order of magnitude.[9,49,71] It is noticed that the value of d is dependent not only on T_r but also on the other experimental conditions such as the pressure during evaporation.[9]

Table 1. The values of the fitted parameters and the measured d. Temperature is in °C, G is in J/(m^3·K) and d is in nm. The films are evaporated unless otherwise noted.

film	Fig.	T_t	T_u / (G)	T_λ / (T_0)	d	d (T_t) of exp. composition
Ni	10			290		∼ 10(RT)
	11	400		250		∼ 50(300)[49]
Fe	13	RT		300	5.4	
Fe–Ni	12	RT	150	300	20	∼ 5(RT),
		250			30	∼ 25(300).
		450			40	81%Ni–Fe[11].
	14	RT			5.5	
		350			22.5	
		450			24	
	18	100		250	20	
				300		
Fe–Ni*	4	250	(12×10^5)	300	30	
Co–Ni	15	RT	400	300	10	10 − 100(200),
		100			11	10 − 100(275),
		320			15	∼ 200(325).
	16				25	50%Co–Ni[71]
	18	100			11	
Fe–Co	17	300	(3×10^5)	300	13	
Fe–Co**		RT		(RT)	40	

*irradiated, **electrodeposited

In conclusion, the magnetization induced anisotropies of Fe–Ni, Ni–Co and Co–Fe films of cubic crystal structure originate from the anisotropy of atomic pair ordering, strain anisotropy and shape anisotropy. For Co and Co-rich Co–Ni and Co–Fe films of hexagonal crystal structure the crystal texture related anisotropy is also an important origin. The anisotropy of Fe films originates mainly from shape

anisotropy and that of Ni films mainly from strain anisotropy. For alloy films the largest contributor to the anisotropy is determined not only by composition fraction but also by T_t. For Fe–Ni alloy films of $T = T_t = \mathrm{RT}$, the largest contributor is K_λ for the Ni concentration fraction larger than 90 %, while for the Ni concentration fraction smaller than 90%, K_u becomes the largest contributor instead. The largest contributor K_u for the films with a composition fraction of about 60% Ni is replaced by K_s if T_t is increased to 450 °C. For 20%−65% Co–Ni films K_u plays a dominant role. For Fe–Co alloy films evaporated at 320 °C K_u is the largest contributor in a Co composition fraction range less than 20% and the strain anisotropy is the largest contributor in a $20\% - 70\%$ Co range. The large spread of K arises mainly from the spread of intrinsic linear stress.

Acknowledgments

Jin Han-Min thanks the Korea Advanced Institute of Science and Technology and Research Center for Advanced Magnetic Materials, Chungnam National University for its invitation through the brain pool project. We are grateful to Professor Han Xiu-Feng and Professor Yan Yu for their help.

References

[1] Blois M S 1955 *J. Appl. Phys.* **26** 975
[2] Francombe M H and Noreika A J 1961 *J. Appl. Phys.* **32** 97S
[3] Kay E 1961 *J. Appl. Phys.* **32** 99S
[4] Wolf I W 1962 *J. Appl. Phys.* **33** 1152
[5] Cohen M S In: Chopra K L (ed) 1969 *Thin Film Phenomena* (New York: McGraw-Hill) p608
[6] Andrä W, Málek Z, Schüppel W and Stemme O 1960 *J. Appl. Phys.* **31** 442
[7] Smith D O, Cohen M S and Weiss G P 1960 *J. Appl. Phys.* **31** 1755
[8] Smith D O 1961 *J. Appl. Phys.* **32** 70S
[9] Pugh E W In: Han G (ed) 1963 *Physics of Thin Films* Vol.1 (New York: Academic) p277
[10] Peng Z L, Han X F, Zhao S F, Wei F X, Du G X and Zhan W S 2006 *Acta Phys. Sin.* **55** 860 (in Chinese)
[11] Wang A L, Liu J T, Zhou Y S, Jiang H W and Zhen W 2004 *Acta Phys. Sin.* **53** 905 (in Chinese)
[12] Blades J D 1959 *J. Appl. Phys.* **30** 260S
[13] Takahashi M, Watanabe D, Kono T and Ogawa S 1960 *J. Phys. Soc. Japan* **15** 1351
[14] Robinson G 1962 *J. Phys. Soc. Japan* **17** Suppl. B-1 558
[15] Graham C D Jr and Lommel J M 1962 *J. Phys. Soc. Japan* **17** Suppl. B-I 570
[16] Takahashi M 1962 *J. Appl. Phys.* **33** 1101
[17] West F G 1964 *J. Appl. Phys.* **35** 1827
[18] Siegle W T and Beam W R 1965 *J. Appl. Phys.* **36** 1721
[19] Wilts C H In: Niedermayer R and Mayer H (ed) 1966 *Basic Problems in Thin Film Physics* (Gottingam: Vandenhoeck and Ruprecht) p422
[20] Wilts C H and Humphrey F B 1968 *J. Appl. Phys.* **39** 1191
[21] Brownlow L W and Wilts C H 1970 *J. Appl. Phys.* **41** 1250
[22] Hoffmann H and Miyazaki T 1974 *IEEE Trans. Magn.* **MAG-10** 556
[23] Tanahashi K and Maeda M 1984 *J. Appl. Phys.* **56** 581
[24] Mitchell E N 1958 *J. Appl. Phys.* **29** 286
[25] Graham C D Jr and Lommel J M 1961 *J. Appl. Phys.* **32** 83S
[26] Segmüller A 1961 *J. Appl. Phys.* **32** 89S
[27] Andrä W and Steenbeck K 1966 *Phys. Stat. Sol.* **17** 191
[28] Smith D O, Weiss G P and Harte K J 1966 *J. Appl. Phys.* **37** 1464
[29] Harte K J, Smith D O, Anderson R M and Johnston R C 1968 *J. Appl. Phys.* **39** 749
[30] Iwata T and Hagedorn F B 1969 *J. Appl. Phys.* **40** 2258
[31] Carbucicchio M, Rateo M, Ruggiero G and Turilli G 2002 *J. Magn. Magn. Mater.* **242–245** 601
[32] Slonczewski J C 1968 *IEEE Trans. Magn.* **MAG-4** 15
[33] Williams C M and Schindler A I 1966 *J. Appl. Phys.* **37** 1468
[34] Srivastava R S 1977 *J. Appl. Phys.* **48** 1355
[35] Néel L 1953 *Comp. Rend.* **237** 1468, 1613
Néel L 1954 *J. Phys. Radium* **15** 225
[36] Taniguchi S and Yamamoto M 1954 *Sci. Rep. Research Insts. Tohoku Univ.* **6** 330
Taniguchi S and Yamamoto M 1955 *Sci. Rep. Research Insts. Tohoku Univ.* **7** 269
[37] Slonczewski J C In: Rado G T and Suhl H (ed) 1963 *Magnetism* Vol.1 (New York: Academic) p205
[38] Ferguson E T 1958 *J. Appl. Phys.* **29** 252
[39] Ignatchenko V A 1961 *Soviet Phys. JETP* **13** 863
[40] Spain R 1963 *Comp. Rend.* **256** 3262
[41] Ruske W and Weber P 1965 *Phys. Stat. Sol.* **12** 321
[42] Jin H M 1983 *J. Magn. Magn. Mater.* **31–34** 931
[43] Smith D O 1959 *J. Appl. Phys.* **30** 264S
[44] Kneer G and Zinn W In: Niedermayer R and Mayer H (ed) 1966 *Basic Problems in Thin Film Physics* (Gottingen: Vandenhoeck and Ruprecht) p437
[45] Kneer G and Zinn W 1966 *Phys. Stat. Sol.* **17** 323
[46] Smith D O and Weiss G P 1965 *J. Appl. Phys.* **36** 962
[47] Lesnik A G, Levin G I and NedostupV M 1966 *Phys. Stat. Sol.* **17** 745
[48] Hanson M, Margitin A and Stjerna B 1995 *J. Magn. Magn. Mater.* **140–144** 701
[49] Néel L 1947 *Comp. Rend.* **224** 1550
[50] Chikazumi S and Oomura T 1955 *J. Phys. Soc. Japan* **10** 842
[51] Chikazumi S 1997 *Physics of Ferromagnetism* 2nd edn (Oxford: Clarendon) p301
Chikazumi S 1964 *Physics of Magnetism* (New York: Wiley) p363
[52] Takahashi M and Kono T 1960 *J. Phys. Soc. Japan* **15** 936

[53] Chikazumi S 1997 *Physics of Ferromagnetism* 2nd edn (Oxford: Clarendon) p324
Chikazumi S 1964 *Physics of Aagnetism* (New York: Wiley) p392
[54] Weast R C 1979- *CRE Handbook of Chemistry and Physics* 60th edn (Boca Raton, FL: CRC Press)
[55] Eckertová L 1986 *Physics of Thin Films* 2nd Revised Edition (New York: Plenum Press)
[56] Murbach H P and Wilman H 1953 *Proc. Phys. Soc.* (London) B **66** 905
[57] Story H S and Hoffman R W 1957 *Proc. Phys. Soc.* (London) B **70** 950
[58] Rymer T B 1956 *Proc. Roy. Soc.* (London) A **235** 274
[59] Puzei I M 1957 *Izv. Acad. Nau. SSSR* **21** 1094 (in Russian)
[60] Lee E W and Asgar M A 1971 *Proc. Roy. Soc.* A **326** 73
[61] Wohlfarth E P In: Wohlfarth E P (ed) 1980 *Ferromagnetic Materials* Vol. 1 (Amsterdam: North-Holland) pp36–37
[62] Bozorth R M 1951 *Ferromagnetism* (Princeton, NJ: Van Nostrand) p662
[63] Brandes E A 1983 *Smithells Metals Reference Book* 6th edn (London: Butterworths)
[64] Van Vlack L H 1985 *Elements of Materials Science and Engineering* (Boston, MA: Addison-Wesley) p163
[65] Goto M, Tange H and Kamimori T 1986 *J. Magn. Magn. Mater.* **62** 251
[66] Málek Z and Schüppel W 1960 *Ann. Physik* **6** 252
[67] Telesnin R V, Saracva I M, Rybak E N and Shishkov A G 1966 *Bull. Acad. Sci. USSR, Phys. Ser.* **30** 102
[68] Uchiyama S, Fujii T, Masuda M and Sakai Y 1967 *Jpn. J. Appl. Phys.* **6** 512
[69] Yamamoto M and Nakamichi T 1958 *J. Phys. Soc. Japan* **13** 228
[70] Chikazumi S 1997 *Physics of Ferromagnetism* 2nd edn (Oxford: Clarendon) p368
Chikazumi S 1964 *Physics of Magnetism* (New York: Wiley) p174
[71] Carter W S 1967 *J. Appl. Phys.* **38** 1347
[72] Humphrey F B and Takahashi M 1965 *J. Appl. Phys.* **36** 963
[73] Takahashi M, Watanabe D, Sasagawa T, Saito H and Ogawa S 1959 *J. Phys. Soc. Japan* **14** 1459
[74] Takahashi M, Watanabe D, Kono T and Ogawa S 1961 *J. Phys. Soc. Japan* **16** 1913
[75] Bozorth R 1951 *Ferromagnetism* (Princeton, NJ: Van Nostrand) p664
[76] Hall R C 1959 *J. Appl. Phys.* **30** 816
Hall R C 1960 *J. Appl. Phys.* **31** 157S
[77] Chikazumi S 1997 *Physics of Ferromagnetism* 2nd edn (Oxford: Clarendon) p368
[78] Lee E W 1955 *Rep. Progr. Phys.* **18** 184
[79] Chikazumi S 1997 *Physics of Ferromagnetism* 2nd edn (Oxford: Clarendon) p361
Chikazumi S 1964 *Physics of Magnetism* (New York: Wiley) p173
[80] Nesbitt E A 1950 *J. Appl. Phys.* **21** 879
[81] Bozorth R 1951 *Ferromagnetism* (Princeton, NJ: Van Nostrand) p663
[82] Bozorth R 1951 *Ferromagnetism* (Princeton, NJ: Van Nostrand) p665
[83] Takahashi M and Kono T 1960 *J. Phys. Soc. Jap.* **15** 936
[84] Jin H M, Kadowaki S and Takahashi M 1986 *J. Magn. Magn. Mater.* **54–57** 917